

# A Hybrid Neural Network and Sugeno-Type Fuzzy Approach for Object Classification to Assist Navigation of Visually Impaired Individuals Using Ultrasonic Sensor Arrays

---

**Ridwan Solihin**

Department of Electrical Engineering, Politeknik Negeri Bandung,  
Bandung, Indonesia

**Rahmawati Hasanah**

Department of Electrical Engineering, Politeknik Negeri Bandung,  
Bandung, Indonesia

**Budi Setiadi**

Department of Electrical Engineering, Politeknik Negeri Bandung,  
Bandung, Indonesia

**Tata Supriyadi**

Department of Electrical Engineering, Politeknik Negeri Bandung,  
Bandung, Indonesia

**Sudrajat**

Department of Electrical Engineering, Politeknik Negeri Bandung,  
Bandung, Indonesia

**R Wahyu Tri Hartono**

Department of Electrical Engineering, Politeknik Negeri Bandung,  
Bandung, Indonesia

---

**Abstract:** This study proposes a hybrid neural network that integrates a multilayer perceptron (MLP) with optimised Sugeno-type fuzzy reasoning for object classification. The system employs a vertically mounted array of ultrasonic sensors arranged 10 cm apart at heights ranging from 80 cm to 180 cm. Each sensor measures the distance of passing objects, producing eleven readings that capture vertical distance patterns. These readings are processed by an MLP with a single hidden layer of 22 neurones to identify characteristic spatial signatures. A refined similarity-based classification is then performed using an optimised Sugeno-type fuzzy inference system configured with five linguistic variables: Very Low (VL), Low (L), Medium (M), High (H), and Very High (VH). Training and testing were conducted using datasets collected at SLBN-A Citeureup, Cimahi, comprising two object categories: human (visually

---

Correspondents Author:  
Budi Setiadi  
Email: budi.setiadi@polban.ac.id

impaired individuals) and nonhuman (inanimate objects). The model was trained for 100 epochs with a learning rate of 0.001. Experimental results show accuracy exceeding 90%, with the hybrid model outperforming the conventional MLP by 1.83%. This improvement reduces false positives and prevents erroneous obstacle warnings. The integration of fuzzy reasoning also enhances the system's robustness to uncertainty and stabilises decision-making when class boundaries overlap.

**Keywords:** Ultrasonic Sensor, MLP, Fuzzy, Optimisation, Classification.

## Introduction

Educated blind people are essentially equipped with orientation and mobility (O&M) skills to support independence when moving from one point to another in their environment. Typically, practitioners combine these skills with assistive devices like manual canes, adaptive electronic canes, or floor tracks. However, the combination of O&M techniques with these assistive devices still has limitations, as they generally only provide distance information to nearby objects and basic path guidance, without the ability to understand environmental conditions more contextually. As a result, blind people still experience difficulties navigating spaces independently, safely, and efficiently. This condition causes user responses to be more reactive than predictive, increasing the risk of navigation errors in social interactions.

Recent research on navigation assistive systems for blind people shows a trend toward integrating multimodal sensors, adaptive algorithms, and fuzzy logic to improve accuracy, safety, and user experience ([Bhatlawande et al., 2024](#); [Li et al., 2019](#); [Silva & Wimalaratne, 2020](#)). Several studies have proposed indoor navigation systems based on RGB-D cameras and semantic maps to detect dynamic obstacles and plan paths in real time ([Messaoudi et al., 2022](#)). Contextual navigation approaches also use sonar sensors, cameras, and fuzzy logic to adapt to changing environmental conditions ([Bouteraa, 2021](#)). Additionally, wearable technologies such as machine learning-based smart clothing that combines ultrasonic sensors, cameras, and GPS have been developed to detect obstacles and provide dynamic movement directions, thereby improving navigation efficiency and reducing user cognitive load ([Lee et al., 2023](#); [Okolo et al., 2025](#)).

Comprehensive studies have shown that single-sensor systems, such as LiDAR, cameras, or ultrasonic sensors, are still limited in detecting moving objects, recognising the direction of arrival, and adapting to varying environmental conditions ([Barontini et al., 2021](#); [Qiu et al., 2020](#); [Tian et al., 2021](#)). Therefore, multi-sensor fusion combined with adaptive fuzzy logic is a more effective approach in handling data uncertainty and generating real-time context-based decisions ([Kleinberg et al., 2023](#)). Furthermore, the integration of sensory and haptic technologies, such as egocentric vision, vibrotactile feedback, and wearable haptic systems, is

being used to enhance users' spatial perception both indoors and outdoors ([Setiadi et al., 2020](#); [Solihin et al., 2023](#); [Supriyadi et al., 2020](#)). In Indonesia, the development of adaptive assistive devices is carried out through technology transfer of smart canes and neural network-based navigation systems to expand the mobility of visually impaired students in special schools ([Supriyadi et al., 2021](#)). Furthermore, an intelligent companion robot combining GPS, a camera, and LiDAR is capable of mapping areas and determining its direction of travel independently. GPS determines the starting and destination positions, while the camera and LiDAR recognise objects and construct a spatial representation of the environment ([Zhang et al., 2023](#)). Based on this gap, this research aims to combine an ultrasonic sensor array with a Sugeno-type neuro-fuzzy approach to adaptively detect and classify objects in real-world environments. This approach is expected to support safer and more contextual navigation for people with visual impairments.

The main objective of this research is to develop, design, and implement an object detection and classification system (human or nonhuman) based on an ultrasonic sensor array. The system is designed to be adaptive to prediction uncertainty, accurate, and integrated into mobility assistive devices installed in the environment. The main contribution of this research is the development of a data processing algorithm model using a hybrid MLP with Sugeno fuzzy reasoning optimised through dynamic parameters ( $\alpha_{base}$ ,  $\gamma$ , and singleton values). This article is structured as follows: The Research Method section discusses the hardware and algorithm model used. The Results and Discussion section presents the experimental results and compares the performance of MLP with the hybrid model. The final section concludes the study.

## Research Method

This study uses an experimental approach to develop, design, implement, and test a classification system based on an array of ultrasonic sensors. The system consists of two main components: hardware for distance data acquisition and a processing module based on the hybrid MLP–Fuzzy Sugeno algorithm. An array of 11 ultrasonic sensors is placed vertically to capture distance profiles of objects at various heights. The number of 11 sensors was chosen based on preliminary testing, which indicated that configurations with fewer sensors were unable to form consistent vertical patterns to distinguish between human and nonhuman objects, while adding sensors beyond 11 did not provide significant accurate improvements but increased scanning latency.

## Hardware

The system hardware consists of three main parts: input, data processing, and output, as shown in Figure 1. Eleven ultrasonic sensors are connected to two separate multiplexers for

the trigger and echo paths, thus enabling controlled scanning using a minimal number of microcontroller pins. The microcontroller runs a hybrid MLP–fuzzy algorithm to perform inference from the distance data and generate classification decisions. The classification results are forwarded to the DFmini-Player module, amplified by an amplifier, and finally delivered through the speaker as audio feedback to the user.

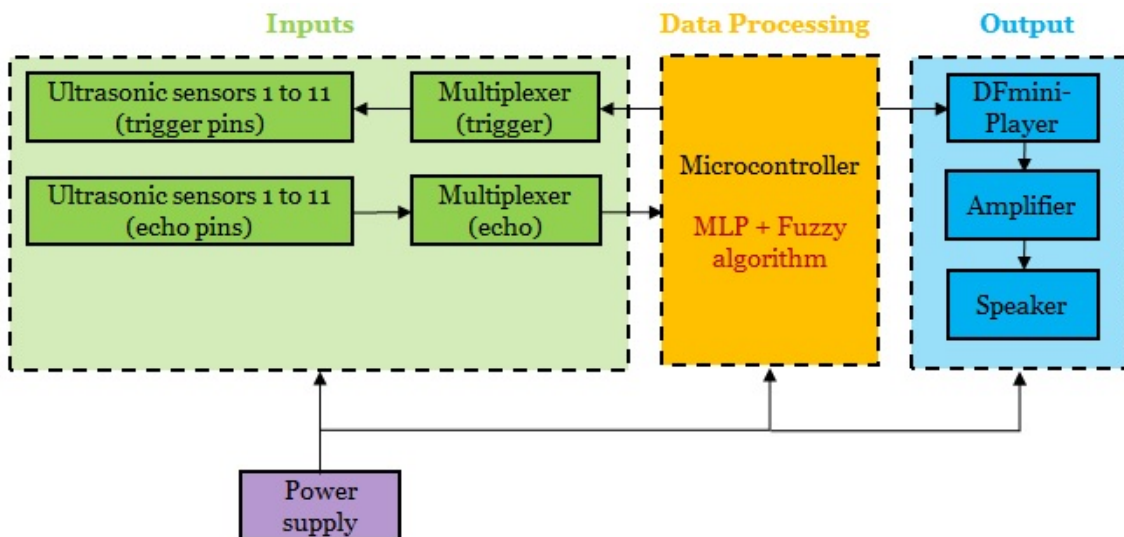


**Figure 1** Hardware Block Diagram

Table 1. presents the hardware pin configuration that connects the CD74HC4067 multiplexer and the DFPlayer Mini module to the microcontroller. MUX A handles the echo path, and MUX B handles the trigger path of the eleven ultrasonic sensors, where the selector pins S0–S3 are mapped together to pins D2–D5 of the microcontroller. The COM pins of MUX A and MUX B are routed to pins D7 and D6, respectively, while the DFPlayer Mini module uses a software serial interface via pins D8 (Rx) and D9 (Tx) to generate audio output.

Table 2. presents the mapping configuration between the ultrasonic sensors and multiplexers in the system. Each HC-SR04 sensor is connected to two CD74HC4067 multiplexers, one each for the Trigger and Echo paths. The trigger paths from the first to the eleventh sensor are allocated sequentially on MUX B channels (CH0–CH10), while the echo paths are mapped in parallel on MUX A channels with the same channel sequence. This architecture allows centralised control of all sensors through two main signal paths, reducing the pin requirements on the microcontroller and simplifying the scanning process. All VCC pins of the sensors and multiplexers are connected to a 5 V supply, while all GND pins are connected to the system ground to maintain a stable voltage reference during data acquisition.

**Table 1 Input/Output Components and Microcontroller Wiring Configuration**

No	Components	Component pins	Microcontroller pins
1	CD74HC4067 (MUX A - Echo)	VCC	5V
		GND	GND
		S0	D2
		S1	D3
		S2	D4
		S3	D5
		COM (SIG)	D7
		EN / INH	GND
2	CD74HC4067 (MUX B - Trigger)	VCC	5V
		GND	GND
		S0	D2
		S1	D3
		S2	D4
		S3	D5
		COM (SIG)	D6
		EN / INH	GND
3	DFPlayer Mini	VCC	5V
		GND	GND
		TX	D8 (Rx for SoftSerial)
		RX	D9 (Tx for SoftSerial)
		SPK1 / SPK2	Speaker

**Table 2 Ultrasonic Sensors and Multiplexer Wiring Configuration**

No	Components	Component pins	Mux pins
1	HC-SR04 #1	Trigger	MUX B CH0
		Echo	MUX A CH0
2	HC-SR04 #2	Trigger	MUX B CH1
		Echo	MUX A CH1
3	HC-SR04 #3	Trigger	MUX B CH2
		Echo	MUX A CH2
4	HC-SR04 #4	Trigger	MUX B CH3
		Echo	MUX A CH3
5	HC-SR04 #5	Trigger	MUX B CH4
		Echo	MUX A CH4
6	HC-SR04 #6	Trigger	MUX B CH5
		Echo	MUX A CH5
7	HC-SR04 #7	Trigger	MUX B CH6
		Echo	MUX A CH6
8	HC-SR04 #8	Trigger	MUX B CH7
		Echo	MUX A CH7
9	HC-SR04 #9	Trigger	MUX B CH8
		Echo	MUX A CH8
10	HC-SR04 #10	Trigger	MUX B CH9
		Echo	MUX A CH9
11	HC-SR04 #11	Trigger	MUX B CH10
		Echo	MUX A CH10

Note: Both VCC pins are connected to the 5V supply, and all GND pins are connected to ground.

## Algorithm

This study develops a hybrid MLP-fuzzy Sugeno auto-tuned algorithm model to improve the accuracy of ultrasonic signal-based object classification. The model is designed to combine the advantages of neural networks that are capable of extracting non-linear representations from numerical data and fuzzy inference systems (FIS) that are capable of imitating human decision-making through linguistic reasoning. Overall, the research stages consist of data acquisition and processing; normalisation; training of the MLP artificial neural network; formation of the Sugeno fuzzy system; and auto-tuning-based hybrid optimisation, as shown in Figure 2.

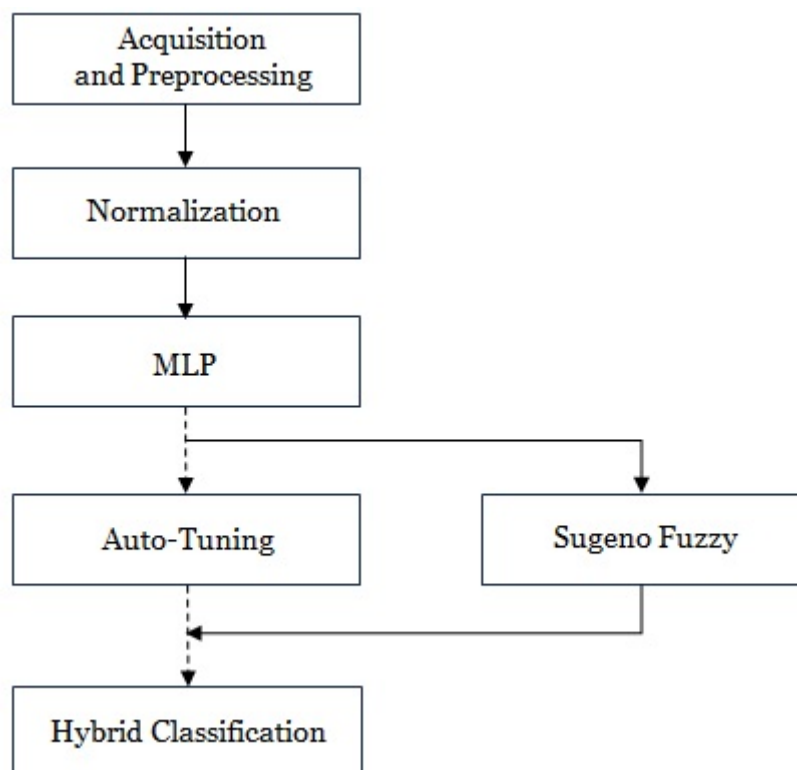


Figure 2 Software Block Diagram

### Data Acquisition and Preprocessing

The dataset consists of distance measurements obtained from 11 ultrasonic sensors, labelled in binary form as human and nonhuman. The dataset is divided into two groups: training data and testing data ([Solihin, 2025](#)). The input variable is denoted as  $X$ , as expressed in Equation (1).

$$X = [x_1, x_2, \dots, x_{11}] \quad (1)$$

where  $x_i$  is the measured distance from the  $i$ -th sensor. The class labels  $y \in \{0,1\}$  represent the nonhuman and human categories, respectively. To ensure stable network training, the data were normalised using the StandardScaler method, as shown in Equation (2), to achieve a

zero-mean and unit-variance distribution. Here,  $\mu$  denotes the mean value, and  $\sigma$  represents the standard deviation of each feature.

$$x' = \frac{x - \mu}{\sigma} \quad (2)$$

## MLP Architecture

The MLP model is designed with 11 input neuronees representing the distance from each sensor, 22 neuronees in the hidden layer, and one binary output neurone, as shown in Figure 3. The selection of 22 neurones is based on the results of an initial evaluation using a simple grid search in the range of 8–32 neurones. The results indicate that 22 neurones provide an optimal balance between accuracy and model complexity. The ReLU activation function (5) is used to accelerate convergence, while the sigmoid  $\sigma$  (6) is used at the output to map the human–nonhuman probabilities. This architecture is designed to approximate a non-linear function that relates the input vector  $X$  to the output probability  $\hat{y}_{MLP}$  (7).  $W_1, W_2, b_1, b_2$  are weights and biases learnt through optimisation using the Adam Optimiser algorithm.

$$z_{1,j} = \sum_{i=1}^{11} w_{1,j,i} x_i + b_{1,j} \quad (3)$$

$$z_{2,k} = \sum_{j=1}^{22} w_{2,k,j} h_j + b_{2,k} \quad (4)$$

$$h_j = f(z_{1,j}) = \text{ReLU}(z_{1,j}) = \max(0, z_{1,j}) \quad (5)$$

$$\sigma(z_2) = \frac{1}{1 + e^{-z_2}} \quad (6)$$

$$\hat{y}_{MLP} = \sigma(W_2 \cdot f(W_1 X + b_1) + b_2) \quad (7)$$

The MLP threshold in this study was set to 0.5. Probability values close to the threshold range [0.4–0.6] result in ambiguous classifications. In such cases, the fuzzy system plays a dominant role in refining the classification outcome. However, for extreme probability values approaching 0 (nonhuman) or 1 (human), the influence of the MLP on the final decision becomes minimal.

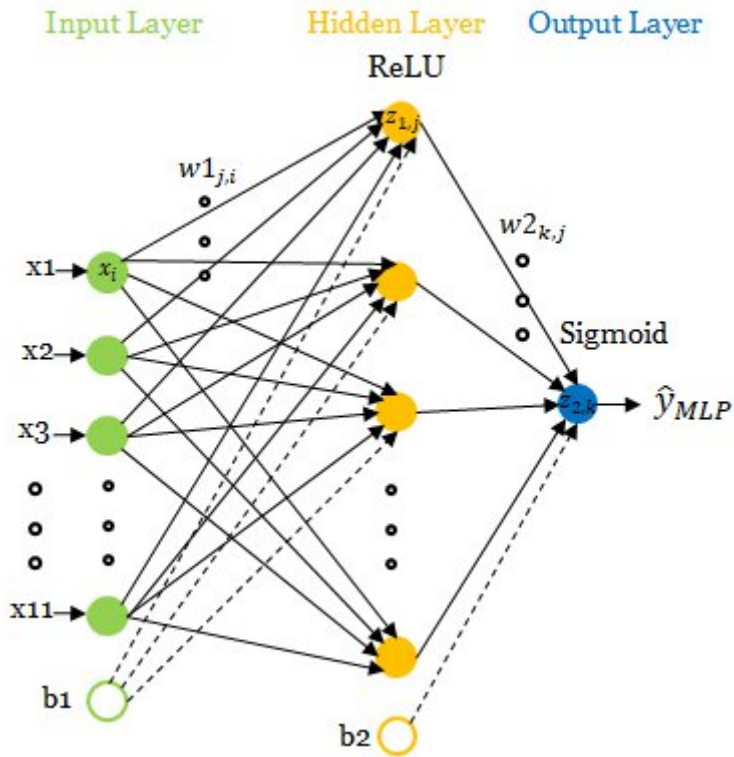


Figure 3 The MLP Model

### Sugeno Fuzzy

The Sugeno Fuzzy System is used to refine the probabilistic classification results of the MLP neural network through a linguistic reasoning-based approach. This model consists of three main stages: fuzzification, inference, and defuzzification. The main objective of integrating Sugeno Fuzzy System in this study is to improve predictions by considering the uncertainty of the MLP results and adding an element of interpretability to the classification process.

In the first stage of fuzzification, five linguistic sets (VL, L, M, H, VH) (8) are selected to map the output probabilities of ( $0 \leq \hat{y}_{MLP} \leq 1$ ) MLP ( $\hat{y}_{MLP}$ ) to the fuzzy domain. The number five is chosen because it provides sufficient resolution to handle areas of ambiguity without excessively increasing the complexity of the rules. The triangular and trapezoidal shapes were chosen because they were computationally efficient and easy to optimise.

$$\text{Linguistic} = \{\text{Very Low (VL), Low (L), Medium (M), High (H), Very High (VH)}\} \quad (8)$$

Each fuzzy set is represented by a triangular or trapezoidal membership function, which determines the extent to which a probability value belongs to a particular linguistic category. The details of the design model for each linguistic VL (9), L (10), M (11), H (12), VH (13).

$$VL = (0, 0, 0.2) \quad (9)$$

$$L = (0.1, 0.2, 0.3, 0.4) \quad (10)$$

$$M = (0.3, 0.5, 0.7) \quad (11)$$

$$H = (0.6, 0.7, 0.8, 0.9) \quad (12)$$

$$VH = (0.8, 1, 1) \quad (13)$$

The definition of searching for the membership degree value  $\mu$  uses triangular (14) and trapezoidal (15) types. For each MLP output probability value ( $\hat{y}_{MLP}$ ), the system calculates the membership degree  $\mu_{VL}, \mu_L, \mu_M, \mu_H, \mu_{VH}$  for the five fuzzy sets.

$$\mu_A(x) = \begin{cases} 0, & x \leq a \\ \frac{x-a}{b-a}, & a < x \leq b \\ \frac{c-x}{c-b}, & b < x \leq c \\ 0, & x \geq c \end{cases} \quad (14)$$

$$\mu_B(x) = \begin{cases} 0, & x \leq a \\ \frac{x-a}{b-a}, & a < x \leq b \\ 1, & b < x \leq c \\ \frac{d-x}{d-c}, & c < x \leq d \\ 0, & x \geq d \end{cases} \quad (15)$$

The second stage of fuzzy inference, a rule-based decision-making process that describes the logical relationship between input and output fuzzy sets. This study uses the 0th-order Sugeno model with rule  $R_i$ (16), where the output of each fuzzy rule is a numeric constant called a singleton. The details of the fuzzy rules used as a model consist of five rules (R1-R5) as shown in Table 3. The  $A_i$  is the fuzzy label of the input and  $s_i$  is a singleton value (numerical constant).

$$\text{LinguR}_i: \text{IF } \hat{y}_{MLP} \text{ IS } A_i \text{ THEN } y_i = s_i \quad (16)$$

**Table 3 Rule Design Model and Singleton Output**

Rules	If ... Then .....	Condition	Singleton
R1	If $\hat{y}_{MLP}$ is VL Then $y_i = s_i$	$0.0 \leq \hat{y}_{MLP} \leq 0.2$	0.00
R2	If $\hat{y}_{MLP}$ is L Then $y_i = s_i$	$0.1 \leq \hat{y}_{MLP} \leq 0.4$	0.30
R3	If $\hat{y}_{MLP}$ is M Then $y_i = s_i$	$0.3 \leq \hat{y}_{MLP} \leq 0.7$	0.60
R4	If $\hat{y}_{MLP}$ is H Then $y_i = s_i$	$0.6 \leq \hat{y}_{MLP} \leq 0.9$	0.85
R5	If $\hat{y}_{MLP}$ is VH Then $y_i = s_i$	$0.8 \leq \hat{y}_{MLP} \leq 1.0$	1.00

The degree of rule activation  $R_i$  is calculated from the membership value of the fuzzy function in the previous stage. Then, each rule contributes to the overall inference result calculated using a weighted average approach (18). The value  $n = 5$  indicates the number of fuzzy rules, and  $\epsilon$  is a positive arbitrary constant with a very small value to avoid division by zero.

$$w_i = \mu_{A_i}(\hat{y}_{MLP}) \quad (17)$$

$$y_{FIS} = \frac{\sum_{i=1}^n w_i s_i}{\sum_{i=1}^n w_i + \varepsilon} \quad (18)$$

The third stage of defuzzification is carried out using a direct method through the calculation of the weighted average (18). The defuzzification result value ( $y_{FIS}$ ) is a single crisp (numeric) number that describes the results of the fuzzy system decision based on the combination of active rules.

### Fuzzy Integration Optimisation in Hybrid Systems

The fuzzy Sugeno output ( $y_{FIS}$ ) is not used separately, but rather adaptive optimization is performed with the MLP results through dynamic weights  $\alpha_{dyn}$ . This integration aims to balance the probabilistic reliability of the MLP with the stability of fuzzy inference against data uncertainty. The hybrid integration equation (19) and dynamic weights  $\alpha_{dyn}$ (20).

$$y_{Hybrid} = \alpha_{dyn} \cdot \hat{y}_{MLP} + (1 - \alpha_{dyn}) \cdot y_{FIS} \quad (19)$$

$$\alpha_{dyn} = \text{clip}(\alpha_{base} + \gamma \cdot |\hat{y}_{MLP} - 0.5|, 0, 1) \quad (20)$$

Parameter  $\alpha_{base}$  controls the level of contribution of the MLP model to the final decision, while  $\gamma$  adjusts the dynamic sensitivity to prediction uncertainty. The range of values for both parameters is arbitrary  $\alpha_{base} = [0.1 - 0.9]$  and  $\gamma = [0.5 - 2.0]$ , while for singletone it is made into three candidates  $[0.0, 0.25, 0.5, 0.75, 1.0]$ ,  $[0.0, 0.3, 0.6, 0.85, 1.0]$ , and  $[0.0, 0.2, 0.4, 0.8, 1.0]$ . Both parameters are optimised through an auto-tuning grid search algorithm, while the singleton value  $[s_1, s_2, s_3, s_4, s_5]$  is adjusted to produce optimal accuracy on the highest validation data. The auto-tuning results selected a combination of  $\alpha_{base} = [0.4]$ ,  $\gamma = [1.2]$ , and singletone  $[0.0, 0.3, 0.6, 0.85, 1.0]$  because it provided the best accuracy on the validation data. The selection of these values refers to the algorithmic tendency where the middle value (M, H) is more sensitive to probability shifts close to the threshold.

## Results and Discussion

This section presents a more in-depth analysis of the results, focusing on the characteristics of the classification errors and their practical implications for use in real-world environments. The research dataset was obtained through a direct acquisition process from ten visually impaired subjects at SLBN-A Citeureup, Cimahi City, as shown in Figure 4. This revision strengthens the analysis by adding interpretations of model failures, potential causes, and their impact on the navigation assistance system.

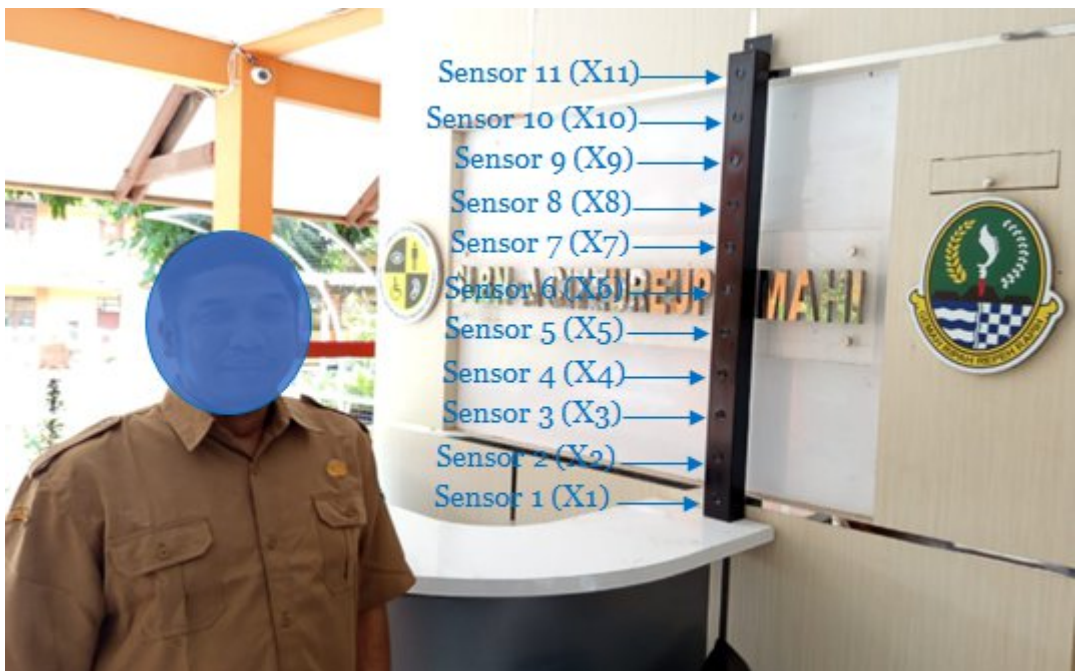


**Figure 4 Dataset and Testing**

The dataset was divided into two subsets using a stratified sampling approach to maintain a representative class distribution, with 1,400 data sets (70%) used for training and 600 data sets (30%) allocated for testing. System evaluation was conducted in two main stages. In the first stage, a single MLP model was tested to gauge the neural network's ability to extract and recognise multidimensional patterns in ultrasonic sensor signals. In the second stage, a hybrid MLP–Fuzzy Sugeno model was evaluated to assess the contribution of the fuzzy inference mechanism in refining the MLP's probabilistic output, particularly through rule-based adjustments designed to improve classification accuracy under conditions of ambiguity. This two-stage approach allows for a more comprehensive comparative analysis between the performance of the conventional model and the fuzzy logic-based hybrid model.

## MLP Training

The MLP model training results show that the learning process is stable and converges well. The training and validation loss curves show a sharp decline in the first 20 epochs, then decrease more slowly until they approach a minimum value at the end of the 100th epoch, as shown in Figure 5. No divergence is observed between the two curves, indicating that the model is not overfitting.

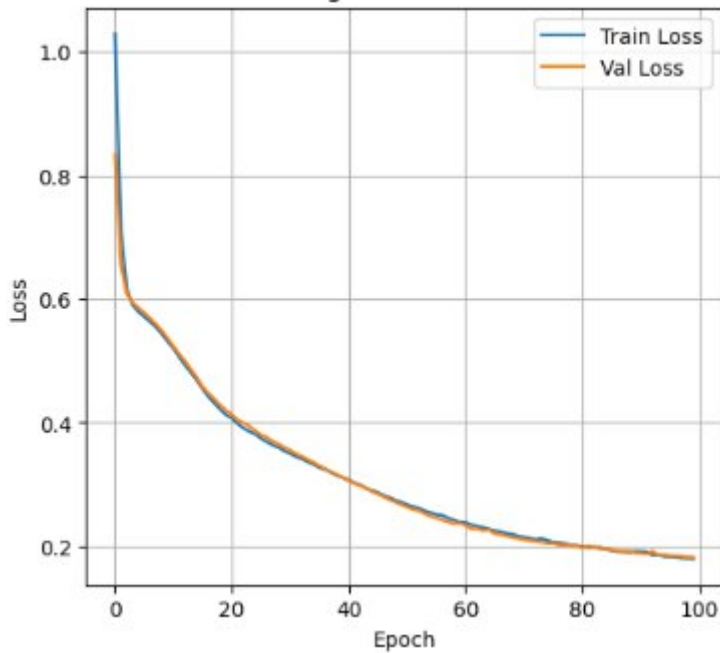


**Figure 5 Training and Validation Loss**

Meanwhile, the accuracy improvement is consistent, where the training accuracy and validation accuracy values increase from around 0.6 at the beginning of training to exceed 0.9 at the end of the epoch, as shown in Figure 6. The difference between the two is relatively small ( $<0.01$ ), which indicates a balance between the learning and generalization capabilities of the model. This condition indicates that the model is able to capture the characteristics of sensor data patterns effectively.

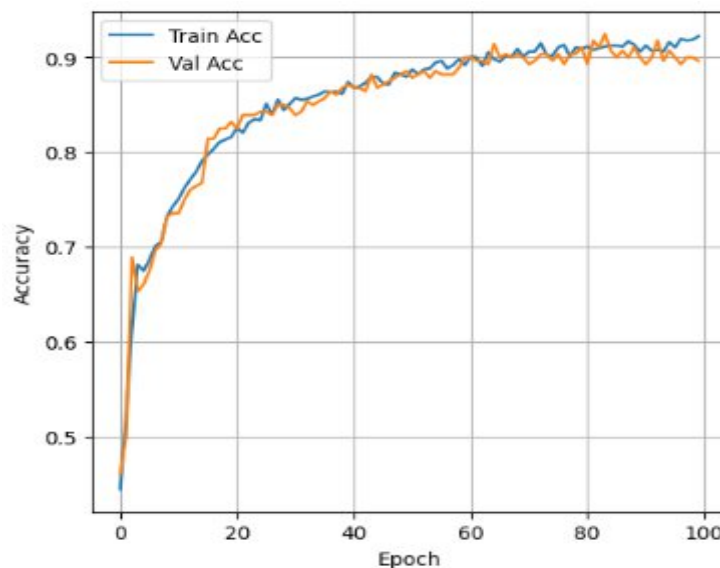


**Figure 6 Training and Validation Accuracy**

## MLP Testing

Based on the test results, a confusion matrix was obtained as shown in Figure 7. True Negative (TN) of 281 indicates the number of non-human class data that were successfully classified correctly, while False Positive (FP) of 30 indicates the number of non-human data that were incorrectly classified as human. Meanwhile, False Negative (FN) of 23 represents undetected human data, and True Positive (TP) of 266 represents correctly classified human data.

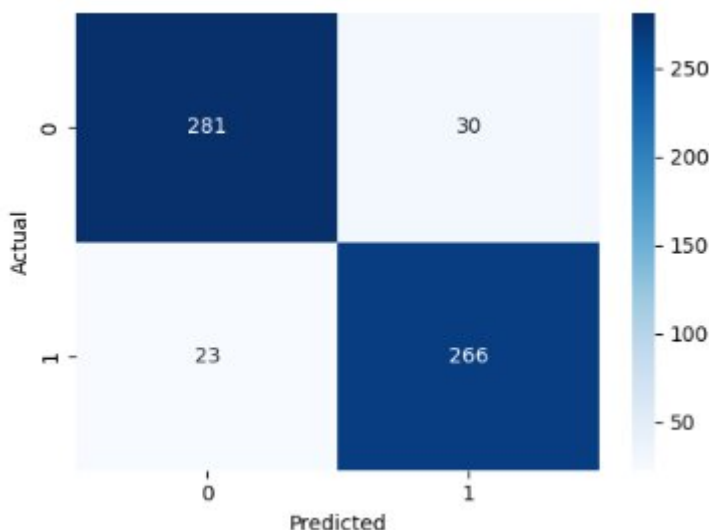


**Figure 7 MLP Confusion Matrix**

Based on the matrix, the MLP model produced an accuracy of 91.17%, a precision of 89.86%, a recall of 92.04%, and an F1-score of 90.94%. These values indicate that the MLP model is capable of performing classification with relatively good performance and a balance between the ability to detect positive and negative classes. However, there is still a fairly high misclassification rate in the non-human class ( $FP = 30$ ), which indicates that the decision boundary (threshold) in the MLP output layer is too rigid to the variation in output probabilities. This condition demonstrates the limitations of MLP in handling data with a high degree of ambiguity or overlap between classes. This phenomenon often occurs when the sensor spacing pattern exhibits vertical contours resembling the human body, such as a high-backed chair or an object with an unevenly reflecting ultrasonic surface.

The ROC curve shows a high AUC, indicating strong class separation ability, as shown in Figure 9. However, the probability zone of 0.4–0.6 represents an area of significant overlap where MLP struggles to make a definitive decision.

## Hybrid Testing

The hybrid model test results produced a confusion matrix as shown in Figure 8. Based on these results, an accuracy of 93.00%, precision of 95.57%, recall of 89.62%, and F1-score of

92.50% were obtained. There was a significant increase in the precision value, indicating that the system is more selective in determining the positive class. Although there was a slight decrease in the recall value (from 92.04% to 89.62%), this decrease was minor and still within the system's tolerance range.

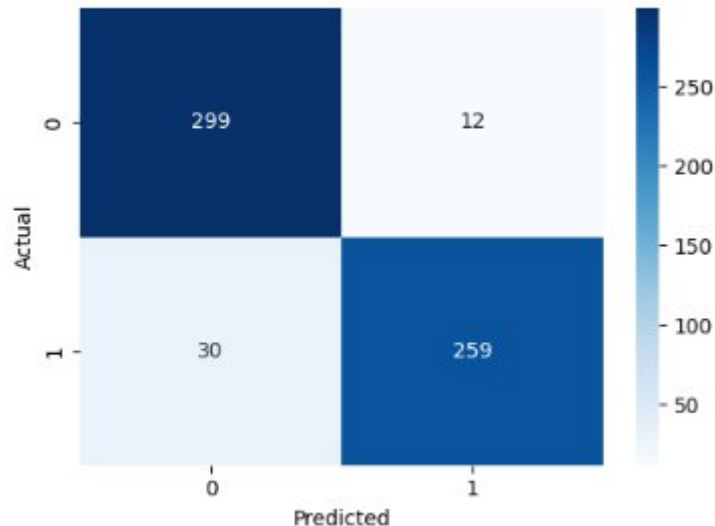


**Figure 8 Hybrid Confusion Matrix**

In addition, the Area Under Curve (AUC) value of 0.9829 indicates a very good and stable class separation capability, as shown in Figure 9. This shows that the fuzzy mechanism is able to refine the classification process carried out by MLP by adding a decision-making layer based on membership degrees, not just binary decisions.

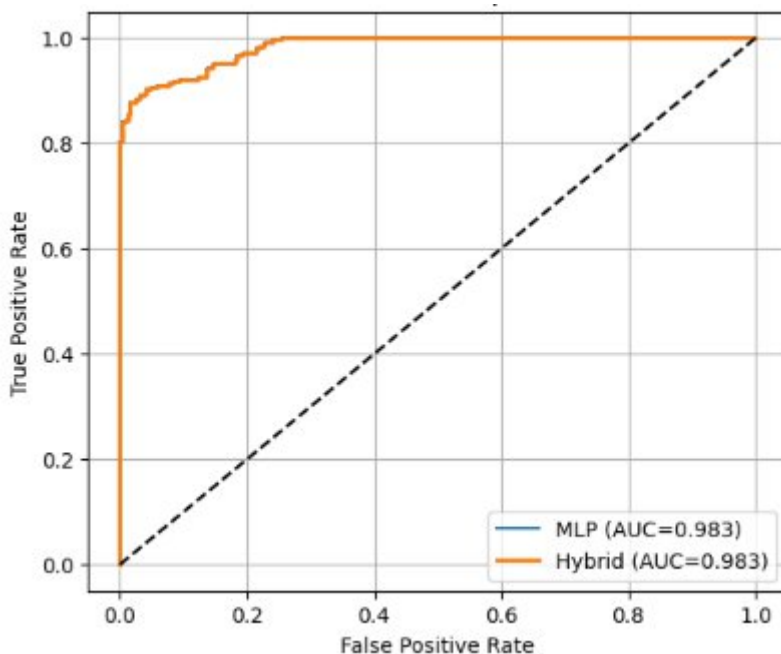


**Figure 9 ROC Curve Comparison**

## Comparative Analysis

This study demonstrates a distinctive methodological improvement compared with related works, summarised in Table 4. The vertical configuration of eleven HC-SR04 sensors provides a richer height-based spatial signature than single-sensor or small-array ultrasonic systems and achieves more stable discrimination of human and non-human objects in variable environments. In contrast, vision-based approaches (Li et al., 2019), (Zhang et al., 2023) offer high accuracy for static and dynamic scenes but remain sensitive to illumination and require higher computational resources. Context-aware or multimodal systems (Silva & Wimalaratne, 2020), (Okolo et al., 2025) improve robustness, yet their performance depends strongly on infrastructure and sensor visibility. Thus, the proposed ultrasonic-based architecture provides a practical balance between robustness, cost, and computational efficiency for wearable navigation assistance.

From an algorithmic standpoint, the hybrid MLP–Fuzzy Sugeno model combined with adaptive weighting ( $\alpha_{\text{base}}$  and  $\gamma$ ) yields a clear performance advantage over conventional MLP and earlier fuzzy-based systems (Bouteraa, 2021). The model achieves a 1.83% accuracy improvement and a 5.71% precision gain relative to standard MLP, driven by the ability of Sugeno inference to refine MLP output probabilities in ambiguous boundary regions. Acting as a decision refiner, the fuzzy layer applies non-linear membership functions and weighted rules to stabilise classification outcomes, effectively reducing false positives without degrading performance in other classes. This adaptive inference mechanism is not present in prior neuro-fuzzy implementations that rely on static rule sets or non-adaptive fusion.

The evaluation results further highlight the strength of this approach, utilising 2,000 field samples collected from ten subjects, larger and more realistic than datasets in fuzzy-based prototypes or small-scale sensor-fusion studies. The model attains 93.00% accuracy, 95.57% precision, and 89.62% recall, representing an acceptable trade-off where the slight reduction in recall is outweighed by substantial false-positive suppression. For navigation assistance, minimising unnecessary alerts is directly linked to user comfort and trust, making precision a critical performance metric. Overall, the proposed hybrid model provides a competitive balance of accuracy, stability, and practicality, outperforming earlier ultrasonic, fuzzy, and multimodal references in its target application domain.

Table 4 Comparatif Comparison

Author	Sensors	Method	Data / Experiment	Results
( <a href="#">Solihin et al., 2025</a> )	11× HC-SR04 (vertical, 10 cm spacing)	MLP (11–22–1) + Sugeno-Fuzzy (5 linguistics) + adaptive weighting ( $\alpha_{base}$ , $\gamma$ )	2,000 field samples (10 subjects), 70/30 split	Accuracy 93.00%, precision 95.57%, recall 89.62%; accuracy improvement 1.83% vs MLP; focus on FP reduction.
( <a href="#">Li et al., 2019</a> )	Camera / RGB (vision)	Vision + semantic mapping	Indoor (public) study	The vision method is strong for static/dynamic objects but vulnerable to lighting; it does not focus on ultrasonic.
( <a href="#">Silva &amp; Wimalaratne, 2020</a> )	Multimodal (context sensors)	Context-aware algorithms	Limited literature/experimental study	Emphasises the benefits of multimodal for robustness; a single sensor has limitations in real-world conditions.
( <a href="#">Bouteraa, 2021</a> )	Wearable sensors + fuzzy	Fuzzy decision support	Prototype implementation	The evidence demonstrates that fuzzy enhances uncertainty tolerance and reduces neural integration in certain studies.
( <a href="#">Zhang et al., 2023</a> )	Camera + LiDAR	Visual recognition + control	Prototype robot	The system performs well in mapping and robotics, but it requires more expensive and complex hardware.
( <a href="#">Okolo et al., 2025</a> )	Multimodal (vision+ultra sonic)	Sensor fusion + ML	Small scale evaluation	Demonstrates benefits of fusion; infrastructure/visibility dependent.

## Conclusions

The hybrid MLP–Fuzzy Sugeno model developed in this study demonstrates consistent improvements in accuracy and precision compared to a single MLP model, primarily through a significant reduction in false positives and increased decision stability in regions of ambiguity. These results confirm the effectiveness of fuzzy reasoning integration in refining

the probabilistic output of neural networks, particularly in ultrasonic sensor-based applications with high levels of uncertainty. However, system performance is still affected by dynamic environmental conditions, such as multiple reflections in narrow corridors, varying angles of incidence of objects, and changes in the physical conditions of the environment that can disrupt measurement reliability. These results indicate that the developed system has the potential to be applied to navigation aids for people with visual impairments in an adaptive and real-time manner. In the future, it is recommended that the system be integrated with multimodal sensors, supported by edge computing and fuzzy adaptive tuning to improve processing speed and adaptability to changing environmental conditions.

## References

Barontini, F., Catalano, M. G., Pallottino, L., Leporini, B., & Bianchi, M. (2021). Integrating Wearable Haptics and Obstacle Avoidance for the Visually Impaired in Indoor Navigation: A User-Centered Approach. *IEEE Transactions on Haptics*, 14(1), 109-122. <https://doi.org/10.1109/TOH.2020.2996748>

Bhatlawande, S., Borse, R., Solanke, A., & Shilaskar, S. (2024). A Smart Clothing Approach for Augmenting Mobility of Visually Impaired People. *IEEE Access*, 12, 24659-24671. <https://doi.org/10.1109/ACCESS.2024.3364915>

Bouteraa, Y. (2021). Design and Development of a Wearable Assistive Device Integrating a Fuzzy Decision Support System for Blind and Visually Impaired People. *Micromachines*, 12(9), 1082. [https://doi.org/https://doi.org/10.3390/mi12091082](https://doi.org/10.3390/mi12091082)

Kleinberg, D., Yozevitch, R., Abekasis, I., Israel, Y., & Holdengreber, E. (2023). A Haptic Feedback System for Spatial Orientation in the Visually Impaired: A Comprehensive Approach. *IEEE Sensors Letters*, 7(9), 1-4. <https://doi.org/10.1109/LSENS.2023.3307068>

Lee, K., Shrivastava, A., & Kacorri, H. (2023). Leveraging Hand-Object Interactions in Assistive Egocentric Vision. *IEEE Transactions on Pattern Analysis and Machine Intelligence*, 45(6), 6820-6831. <https://doi.org/10.1109/TPAMI.2021.3123303>

Li, B., Muñoz, J. P., Rong, X., Chen, Q., Xiao, J., Tian, Y., Ardit, A., & Yousuf, M. (2019). Vision-Based Mobile Indoor Assistive Navigation Aid for Blind People. *IEEE Transactions on Mobile Computing*, 18(3), 702-714. <https://doi.org/10.1109/TMC.2018.2842751>

Messaoudi, M. D., Menelas, B.-A. J., & McHeick, H. (2022). Review of Navigation Assistive Tools and Technologies for the Visually Impaired. *Sensors*, 22(20), 7888. <https://doi.org/https://doi.org/10.3390/s22207888>

Okolo, G. I., Althobaiti, T., & Ramzan, N. (2025). Smart Assistive Navigation System for Visually Impaired People. *Journal of Disability Research*, 4(1). <https://doi.org/10.57197/jdr-2024-0086>

Qiu, S., Hu, J., Han, T., Osawa, H., & Rauterberg, M. (2020). An Evaluation of a Wearable Assistive Device for Augmenting Social Interactions. *IEEE Access*, 8, 164661-164677. <https://doi.org/10.1109/ACCESS.2020.3022425>

Setiadi, B., Supriyadi, T., Nugroho, H., & Solihin, R. (2020). Navigation and Object Detection for Blind Persons Based on Neural Network. *International Journal of Applied Technology Research*, 01, 56-65.

Silva, C. S., & Wimalaratne, P. (2020). Context-Aware Assistive Indoor Navigation of Visually Impaired Persons. *Sensors and Materials*, 32(4). <https://doi.org/10.18494/sam.2020.2646>

Solihin, R. (2025). *Ultrasonic Sensor Data for Human or Nonhuman Classification* Zenodo. <https://doi.org/10.5281/zenodo.17570810>

Solihin, R., Setiadi, B., Baisrum, B., Siswoyo, S., Al Tahtawi, A. R., & Utomo, T. B. (2023). Technology Transfer and Training on Making Adaptive Sticks to Instructors at SLBN-A Citeureup, Cimahi City to Improve the Mobility Orientation Ability of Students with Visual Disabilities. *REKA ELKOMIKA: Jurnal Pengabdian kepada Masyarakat*, 04, 272-281. <https://doi.org/10.26760/rekaelkomika.v4i3.272-281>

Supriyadi, T., Salsabila, A., Solihin, R., Hanifatunnisa, R., Setiadi, B., & Afni, S. (2021, 2021/11/23). Position Coordination Aid for Blind Persons Based on LoRa Point to Point. Proceedings of the 2nd International Seminar of Science and Applied Technology (ISSAT 2021),

Supriyadi, T., Setiadi, B., & Nugroho, H. (2020, 2020/02/01). Pedestrian lane and obstacle detection for blind people. *Journal of Physics: Conference Series*, 1450(1), 012036. <https://doi.org/10.1088/1742-6596/1450/1/012036>

Tian, S., Zheng, M., Zou, W., Li, X., & Zhang, L. (2021). Dynamic Crosswalk Scene Understanding for the Visually Impaired. *IEEE transactions on neural systems and rehabilitation engineering*, 29, 1478-1486. <https://doi.org/10.1109/TNSRE.2021.3096379>

Zhang, L., Jia, K., Liu, J., Wang, G., & Huang, W. (2023). Design of Blind Guiding Robot Based on Speed Adaptation and Visual Recognition. *IEEE Access*, 11, 75971-75978. <https://doi.org/10.1109/ACCESS.2023.3296066>